

Geospatial Assessment of Urbanization and its Impact on the Thermal Intensity & Seasonal Surface Temperatures - A Case Study on Bangalore

V Prashant Kumar¹, Dr. B Santhaveerana Goud²

¹PG Student, Department of Civil Engineering, UVCE Bangalore, Bangalore, 56056, Karnataka, India

²Professor, Department of Civil Engineering, UVCE Bangalore, Bangalore, 56056, Karnataka, India

Abstract: *The development of urban areas and related landscape changes has been significant contributors to local, regional, and global environmental change. A significant element affecting the characteristic urban heat and its repercussions has been found as the conversion of urban vegetation to impermeable landscapes. The development and maintenance of urban vegetation as heat sinks is sometimes viewed as a waste of space due to the strong demand for real estate in metropolitan settings. Due to these physical changes, such as a decline in green cover and an increase in built - up area in cities, the need for the construction and protection of such areas is growing. As a result, the land surface temperature (LST) will inevitably rise. Urban heat islands may worsen the quality of the environment where people live, increase energy demand, elevate ground level ozone, and potentially raise death rates. Using the recently launched Landsat 8 and MODIS Land Surface and Temperature LST data sets, this study sought to quantify the multi - seasonal heat contribution of major Land Use Land - Cover LULC within these cities. This study demonstrates the value of remotely sensed data sets in understanding the impact of LULC types on the urban microclimate. Designing sustainable urban socio - economic and environmental solutions to address local, regional, and global climate change would benefit significantly from the study.*

Keywords: Geospatial Assessment, Urbanization, Thermal Intensity

1. Introduction

Urbanisation is a type of metropolitan expansion that occurs in reaction to a region's physical topography as well as a variety of frequently perplexing economic, social, and political variables. It is the rise of urban populations relative to rural population in the area. Villages turn into towns, and towns turn into cities, and cities turn into metropolises as a result of the urbanisation process, which is aided by infrastructural improvements, population expansion that follows, and migration. In terms of infrastructure development, traffic congestion, and the provision of basic amenities (such as electricity, water, and sanitation), urbanisation and urban sprawl have presented serious challenges to those in charge of city planning and management (Kulkarni and Ramachandra, 2006). In addition, the following are significant effects of urbanisation:

- **Heat island:** Surface and atmospheric temperatures are raised as a result of human - caused heat discharge from energy use, increased use of artificial materials with high heat conductivities and capacities, and a consequent decline in vegetation and permeable surfaces, which would otherwise allow for the evapotranspiration that lowers surface temperatures.
- **Loss of aquatic ecosystems:** Urbanization has significant effects on natural resources, such as a decrease in the quantity of water bodies and/or a lowering of the groundwater level.
- By increasing the amount and rate of surface runoff, unplanned urbanisation has significantly changed the drainage characteristics of natural catchments, or drainage regions. Because of the careless dumping of solid waste, drainage systems frequently have blockages

and are unable to handle the increased amount of water. Floodways get blocked by the encroachment of wetlands, floodplains, etc., reducing the amount of natural flood storage.

- Utilising a variety of satellite data products gathered in the thermal area of the electromagnetic spectrum, studies on the phenomena of Urban Heat Island (UHI) have been undertaken utilising satellite derived land surface temperature (LST) measurements. Different geographical resolution and temporal coverage data from currently accessible satellite thermal infrared sensors can be utilised to calculate LST.

2. Study Area

Due to Bangalore's pivotal role in the socioeconomic and technical developments that are now taking place at the regional and global levels, Bangalore has been chosen for this research. It is a major hub for the information technology sector globally and draws professionals from all around. The city has a tropical savannah climate and is situated in southern India at 12° 59' north latitude and 77° 57' east longitude. It is 920 metres above mean sea level.

Bangalore experiences yearly rainfall of around 880 mm, summer temperatures of 18 to 38 °C, and winter temperatures of 12 to 25 °C. The vegetation around Bangalore is made mostly of agriculture and grassland (IMD, 2008), with some tropical evergreen and fruit trees and huge, deciduous canopies and parks. Within the municipal limits of Bangalore, there are 117 lakes and tanks in addition to some old parks like Lalbagh and Cubbon Park. The city's physical and cultural landscapes have seen significant change recently as a result of investments in industry, infrastructure, and other services, especially in light

of the water bodies and parks. Due to the 2006 consolidation of eight nearby administrative bodies under Bangalore's municipal authority, the city's population has increased by more than a factor of ten since 1949 (Sudhira et al., 2007). With a population of 7 million, Bangalore is now the sixth biggest metropolitan in India. Open, public places have been getting smaller over time as a result of fast expansion. Numerous thousand roadside trees have been lost due to overcrowding, congestion, and the growth of the city's traffic networks. Additionally, numerous lakes have been encroached upon by residential construction, bus terminals, parks, and stadiums. The city now confronts several fresh environmental concerns as a result of its increased air and sound pollution. There is an urgent need to thoroughly study the influence of urban expansion upon urban temperature since a decline in tree cover may eventually cause an urban heat island to rise in temperature.

3. Data Collection and Methodology

3.1. Data Collection

The USGS's <https://earthexplorer> website was used to download the satellite data used in this study. Lands at 4&5, Lands at 7, Lands at 8 Lands at 9 (OLI/TIRS) from 1993 to 2023 at an interval of 5 years, at a scale of 1: 25000 were used.

3.2. Methodology

Figure 1 shows the complete methodology adopted in the present study.

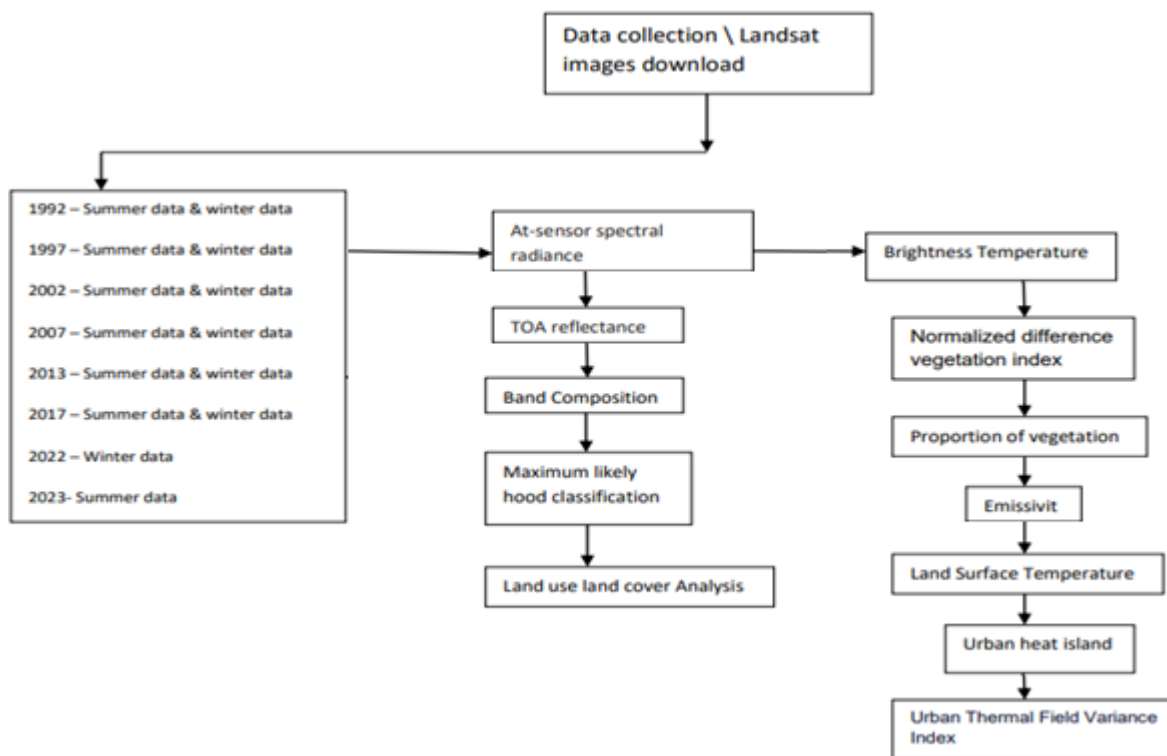


Figure 1: Methodology Flow Chart

Methodology is divided into 3 segments.

- Land use land cover Classification
- Land Surface temperature calculation
- Urban heat island calculation

3.2.1. Land use Land Cover Classification (LULC)

Image classification is a process in which LULC is classified into different classes using multispectral data. As a result, many scholars have introduced several methodologies for supervised classification and unsupervised classification.

3.2.1.1. Conversion to at - sensor spectral radiance (Qcal - to - Lλ) for Landsat – 4, 5&7

$$\text{Spectral radiance } L, \lambda = \text{Grescale} \times \text{Qcal} + \text{Brescal} \quad (1)$$

Where - $L\lambda$ = Spectral radiance at the sensor's aperture watt per steradian per square metre $[W/ (m^2 \text{ sr } \mu\text{m})]$, $Qcal$ = Quantized calibrated pixel value [DN], $Grescale$ = Band - specific rescaling gain factor $[(W/ (m^2 \text{ sr } \mu\text{m})) / \text{DN}]$, $Brescale$ = Band - specific rescaling bias factor $[W/ (m^2 \text{ sr } \mu\text{m})]$.

3.2.1.2. Sensor Spectral Radiance for Landsat 8 & 9

$$\text{Spectral radiance } L\lambda = \text{ML} * \text{Qcal} + \text{AL} \quad (2)$$

Where - $L\lambda$ = Spectral radiance watt per steradian per square metre $(W/ (m^2 * \text{sr} * \mu\text{m}))$, ML = Radiance multiplicative scaling factor for the band ($\text{RADIANCE_MULT_BAND_n}$ from the metadata), AL = Radiance additive scaling factor for the band ($\text{RADIANCE_ADD_BAND_n}$ from the metadata), $Qcal$ = Level 1 pixel value in DN.

3.2.1.3. Conversion to TOA reflectance (L_λ - to - ρ_λ) for Landsat 4 - 7

$$\rho_\lambda = \frac{\pi \cdot L_\lambda \cdot d^2}{ESUN_\lambda \cdot \cos \theta_s} \quad (3)$$

Where - ρ_λ = Planetary TOA reflectance [unitless], π = Mathematical constant equal to ~ 3.14159 [unitless], L_λ = Spectral radiance at the sensor's aperture [$W / (m^2 \text{ sr } \mu m)$], d = Earth-Sun distance [astronomical units], $ESUN_\lambda$ = Mean exo atmospheric solar irradiance [$W / (m^2 \mu m)$], θ_s = Solar zenith angle [degrees].

3.2.1.4. Conversion to TOA reflectance (L_λ - to - ρ_λ) for Landsat 8 & 9

$$\rho_\lambda' = M_p * Q_{cal} + A_p \quad (4)$$

Where - ρ_λ' = TOA Planetary Spectral Reflectance, without correction for solar angle. (Unitless), M_p = Reflectance multiplicative scaling factor for the band (REFLECTANCE_MULT_BAND_n from the metadata), A_p = Reflectance additive scaling factor for the band (REFLECTANCE_ADD_BAND_N from the metadata), Q_{cal} = Level 1 pixel value in DN.

3.2.2. Land Surface temperature calculation (LST).

There are various steps in calculating Land Surface Temperature.

3.2.2.1. Conversion to at - sensor brightness temperature (L_λ - to - BT)

Brightness Temperature BT -

$$T = \frac{K_2}{\ln\left(\frac{K_1}{L_\lambda} + 1\right)} \quad (5)$$

Where - T = Effective at - sensor brightness temperature [K], K_2 = Calibration constant 2 [K], K_1 = Calibration constant 1 [$W / (m^2 \text{ sr } \mu m)$], L_λ = Spectral radiance at the sensor's aperture [$W / (m^2 \text{ sr } \mu m)$], \ln = Natural logarithm.

3.2.2.2. Calculating Normalized difference vegetation index (NDVI).

The traditional method for calculating NDVI is to use a ratio of the red (R) and near infrared (NIR) values: $(NIR - R) / (NIR + R)$

$NDVI = (Band 5 - Band 4) / (Band 5 + Band 4)$ (6)
for Landsat 8 & 9. Where - Band 5 - NIR, Band 4 - R.

$NDVI = (Band 4 - Band 3) / (Band 4 + Band 3)$ (7)
for Landsat 4 to 7. Where - Band 4 - NIR, Band 3 - R.

3.2.2.3. Calculating Proportion of vegetation (Pv).

$$P_v = ((NDVI - NDVI_{min}) / (NDVI_{max} - NDVI_{min}))^2 \quad (8)$$

Where - P_v = Proportion of Vegetation, NDVI = Normalized difference vegetation index.

3.2.2.4. Calculating Land surface emissivity (ϵ).

$$\epsilon = 0.004 * P_v + 0.986 \quad (9)$$

Where - 0.004 - constant, P_v - Proportion of vegetation & 0.986 - corresponds to a correction value of the equation.

3.2.2.5. Calculating Land surface Temperature.

$$LST = (BT / (1 + (\lambda * BT / C_2) * \ln(\epsilon))) \quad (10)$$

Where: BT - Brightness temperature, λ - Central band wavelength which is 11.45 for Landsat 4 - 7 and 10.8 for band 10 & 12.0 for Band 11 on Landsat 8 - 9, C_2 - Constant 14388 & ϵ - Emissivity

3.2.3. Urban Thermal Field Variance Index Calculation

There are two steps that we follow in analysis of Thermal Field variance Index which are.

3.3.3.1. Retrieving of urban heat island (UHI)

$$UHI = LST - LST_m / SD \quad (11)$$

Where - LST = Land Surface Temperature, LST_m = Mean temperature of the Land surface temperature, SD = Standard deviation.

3.3.3.2. Retrieving of Urban thermal field variance index (UTFVI).

$$UTFVI = LST - LST_m / LST \quad (12)$$

Where - LST - Land Surface Temperature, LST_m - Mean Land Surface Temperature.

4. Results

Results have been classified into 3 divisions which are.

4.1. Land use land cover outputs

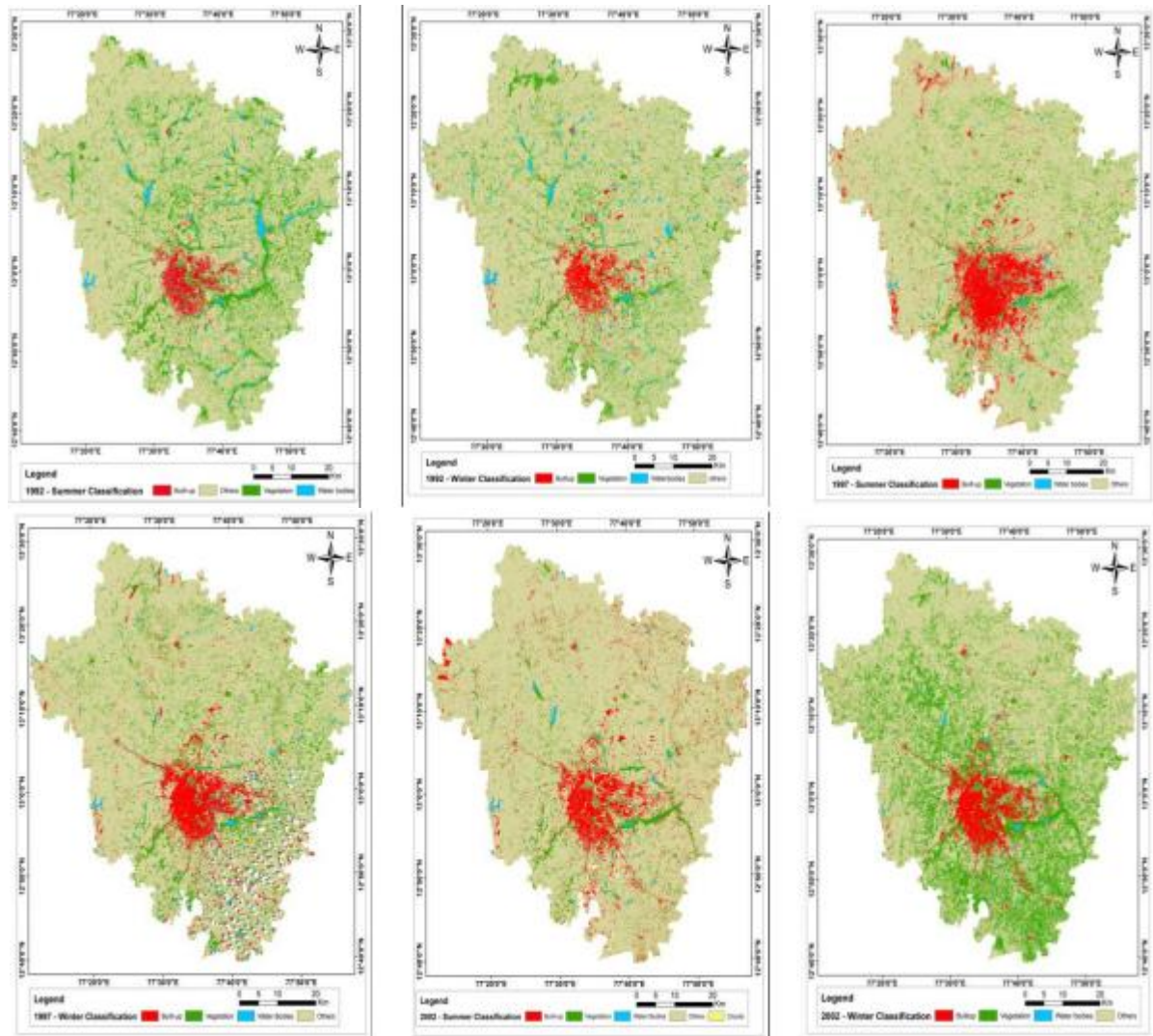
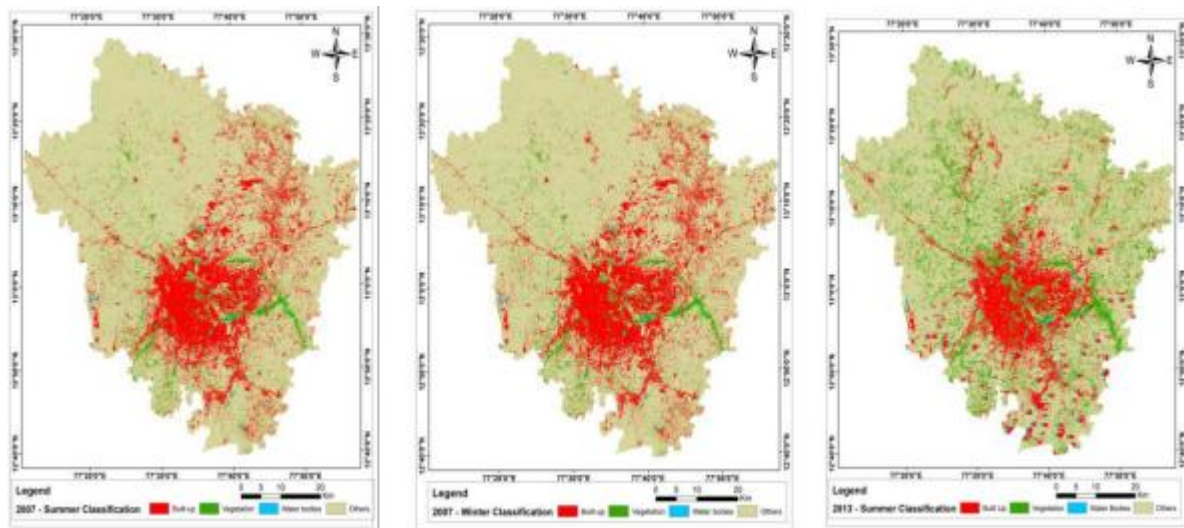


Figure 4.1.1: Summer & winter classification from 1992- 2002



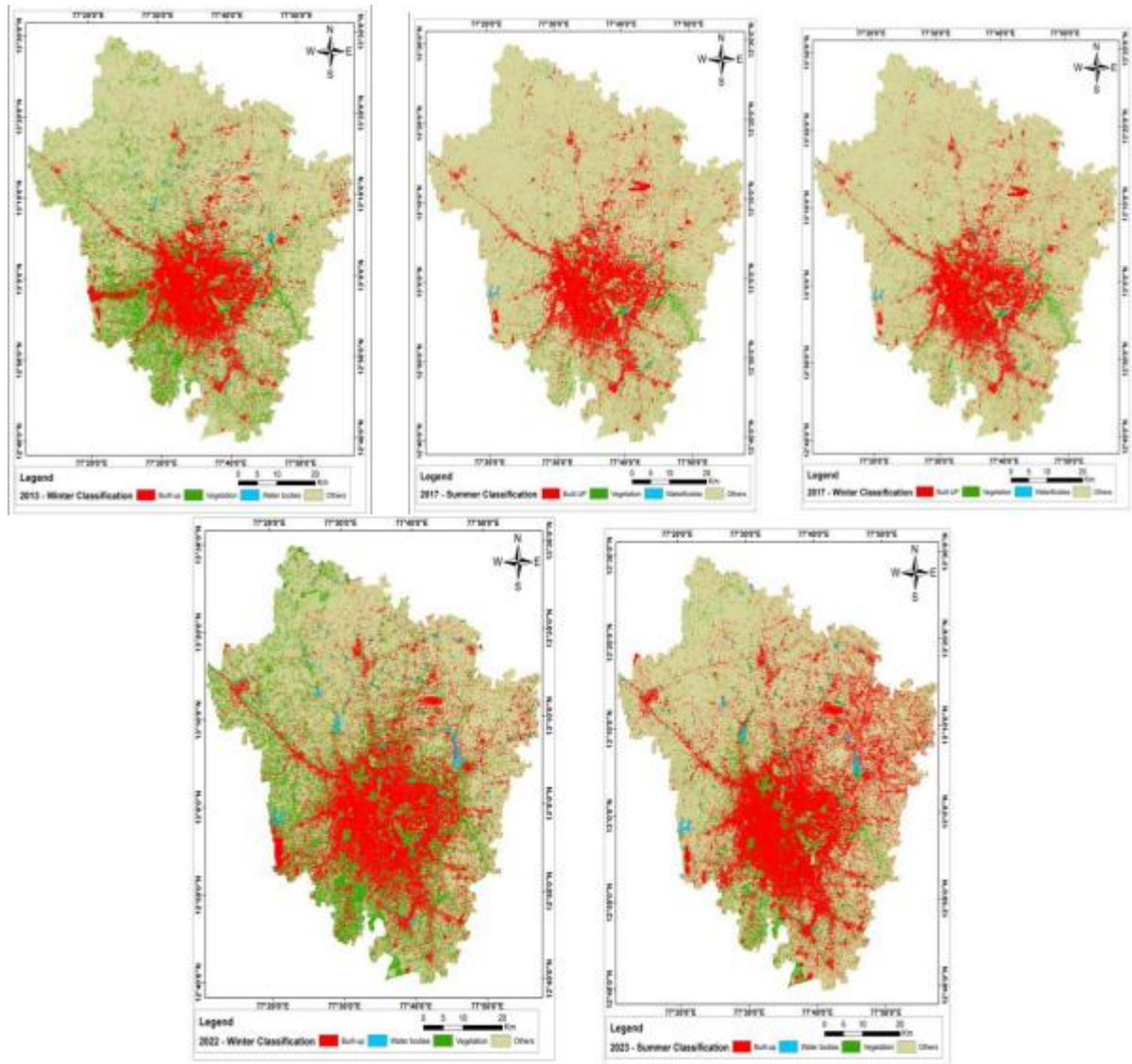


Figure 4.1.2: 1997 Summer & Winter classification from 2007- 2023

4.2. Land Surface Temperature Outputs

Based on **Comfort Index** the results have been classified as follows refer table 4.1.

Table 4.1: Comfort Index

Index number	Comfort index class category	Condition
1	Severe Danger	$WC \leq -35^{\circ}C$
2	Extreme Cold	$-35^{\circ}C < WC \leq -20^{\circ}C$
3	Uncomfortably Cold	$-20^{\circ}C < WC \leq 0^{\circ}C$
4	Cool	$0^{\circ}C < T \leq 15^{\circ}C$
5	Comfortable	$15^{\circ}C < T \leq 25^{\circ}C$
6	Warm	$25^{\circ}C < T \leq 32^{\circ}C$
7	Uncomfortably Hot	$T > 32^{\circ}C$ and $HI \leq 38^{\circ}C$
8	Severe Danger	$HI > 38^{\circ}C$

WC: Wind Chill; T: Temperature; HI: Heat Index.

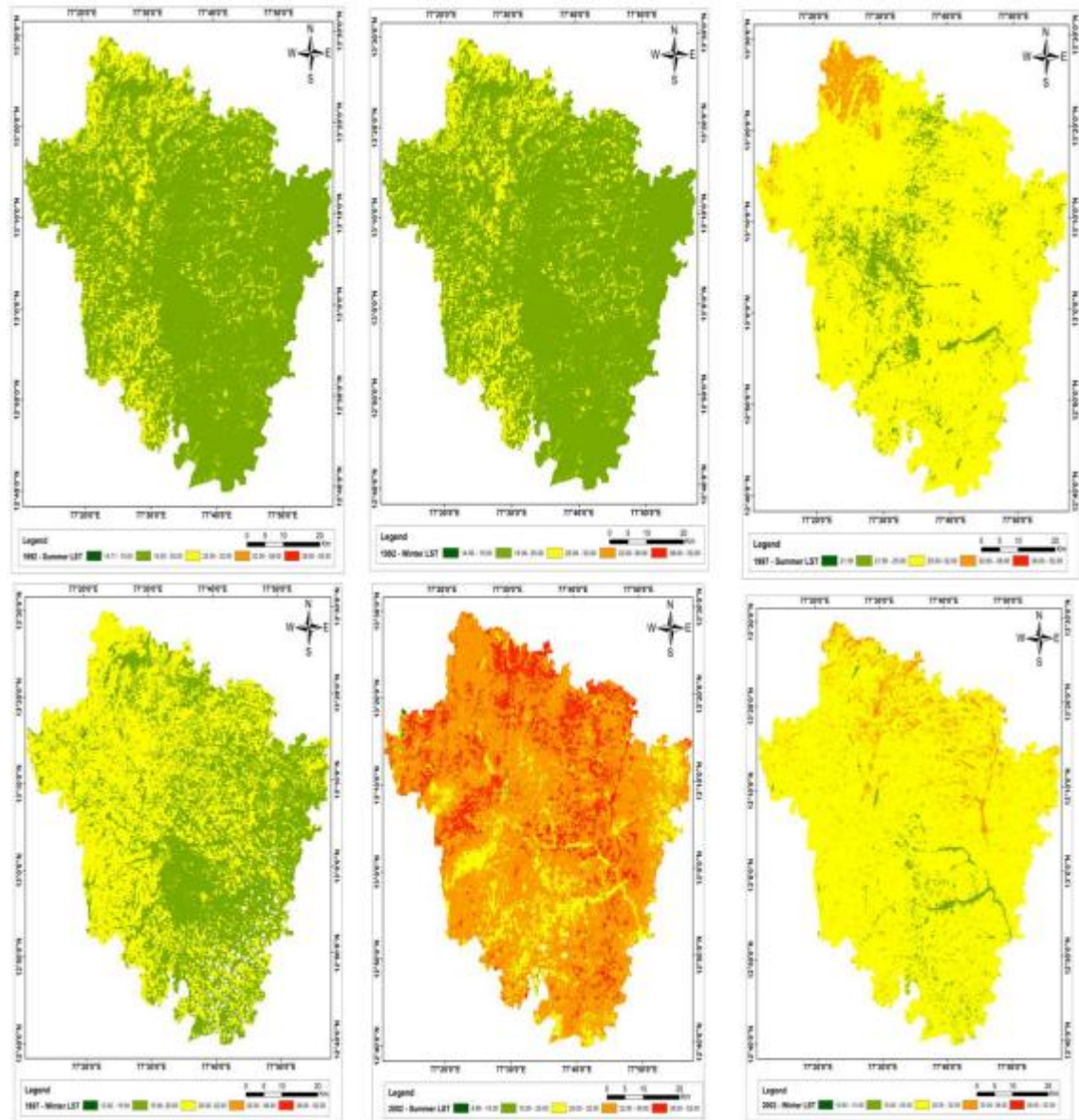
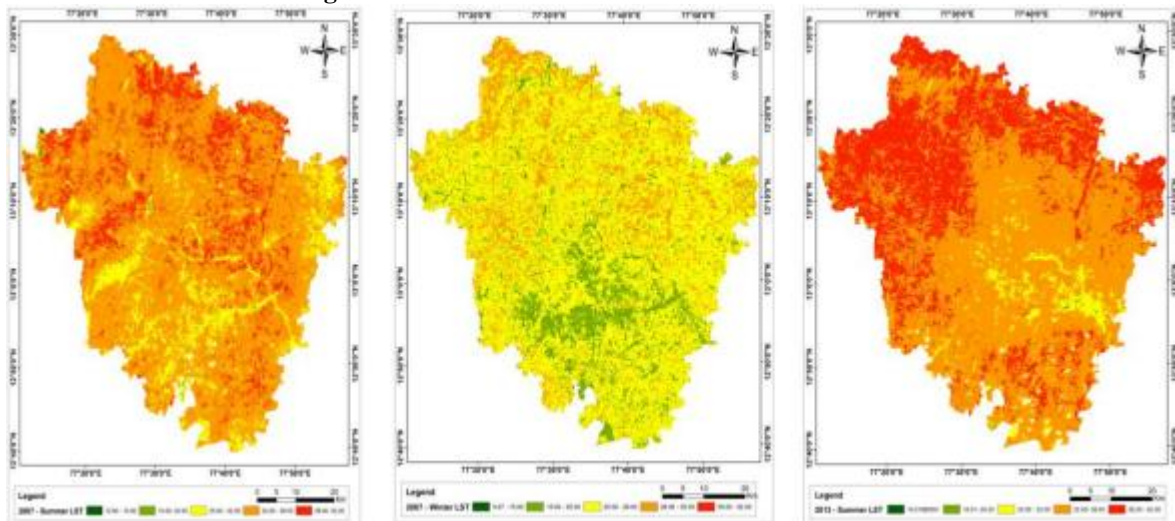


Figure 4.2.1: Summer & winter LST from 1992- 2002



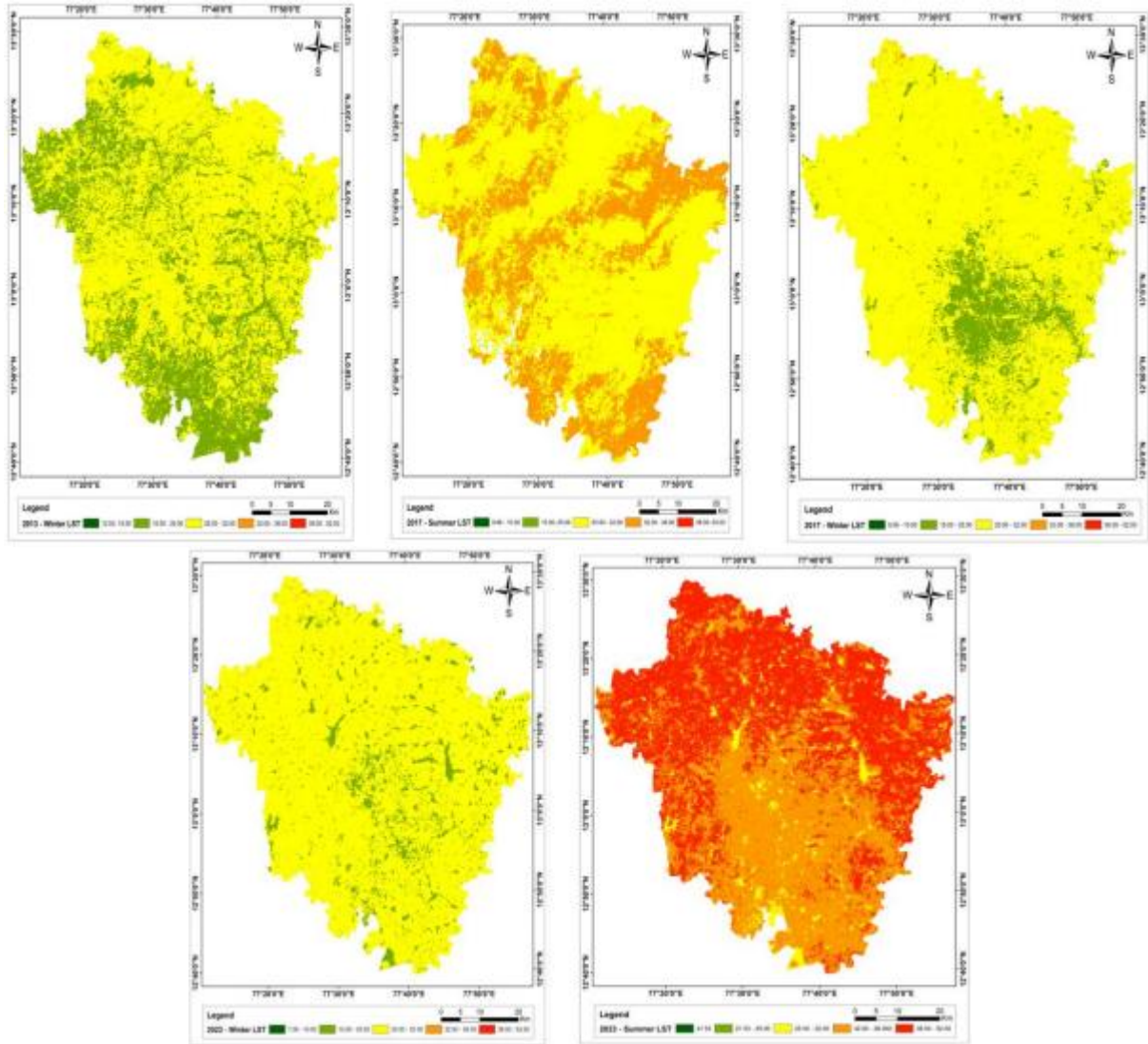


Figure 4.2.2: Summer & winter LST from 2007- 2023

4.3 Urban Thermal Field Variance Index Outputs

With reference to table - 4.2 below UHI Phenomenon has been classified into 6 classifications, refer the table for threshold values.

Table: Threshold Values of UTFVI

UHI Phenomenon		UTFVI	Ecological Evaluation Index
None	Low	<0	Excellent
Weak		0-0.005	Good
Middle	Moderate	0.005- 0.01	Normal
Strong		0.01-.015	Bad
Stronger	High	0.015- 0.02	Worse
Strongest		>0.02	Worst

Table 4.2: Threshold values of UTFVI

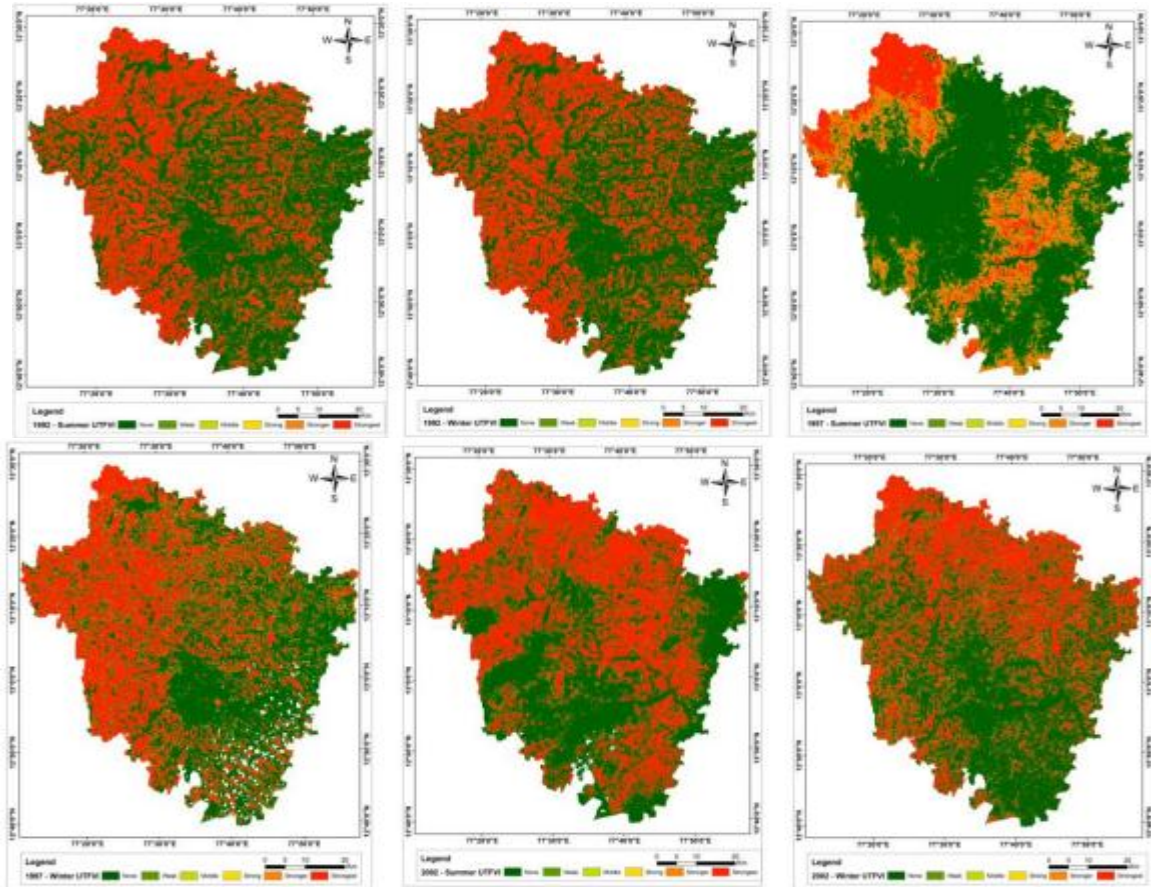
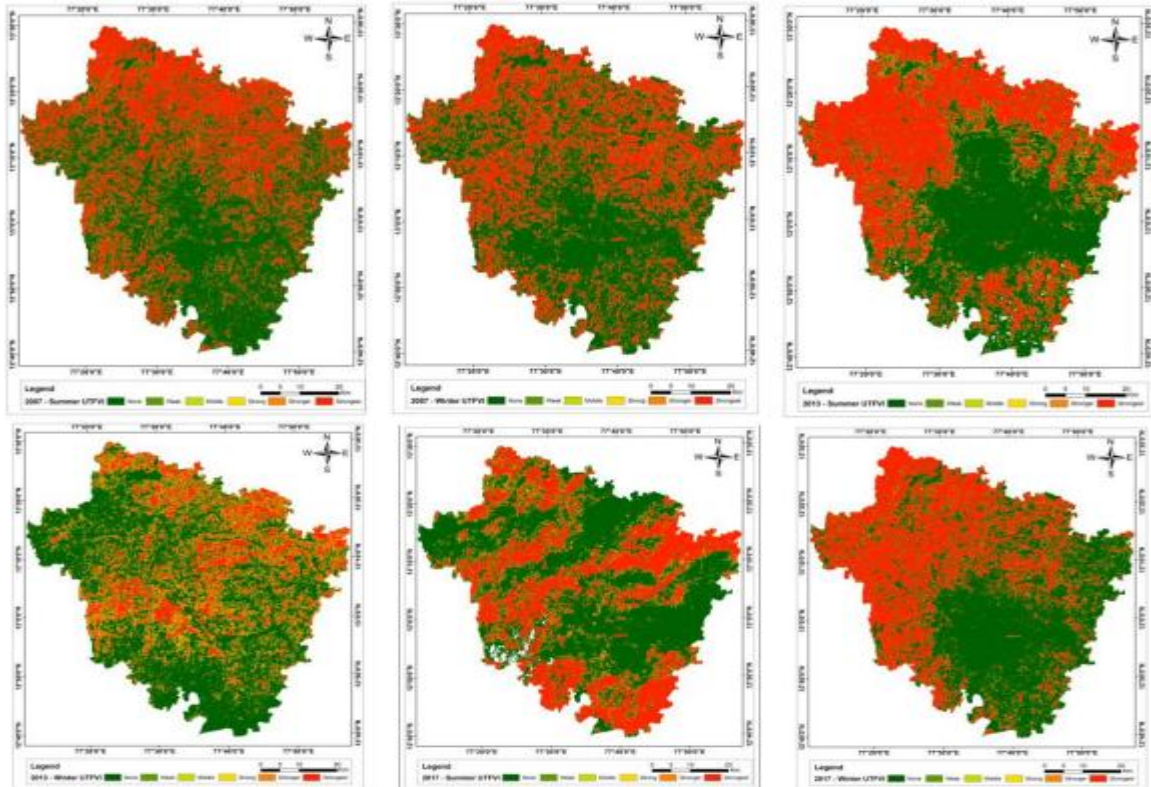


Figure 4.3.1: Summer & Winter UTFVI From 1992 - 2002



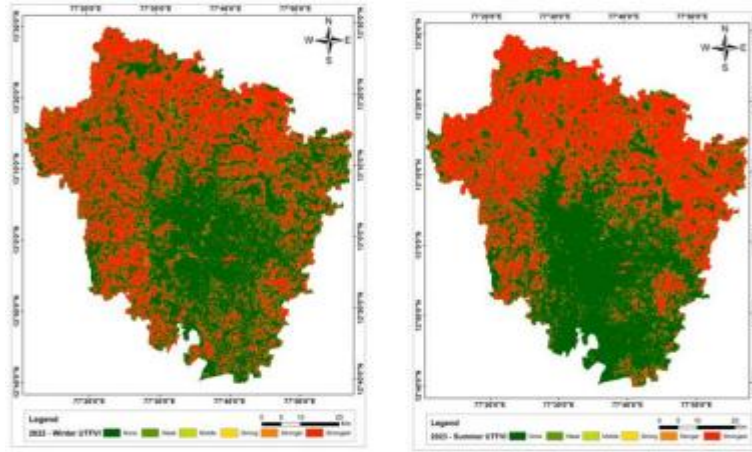


Figure 4.3.2: Summer & Winter UTFVI From 2007 – 2023

5. Observations and Preventive Measures

5.1 Observations

With reference to below table – 5.1 & table- 5.2, we can see 10 % raise in built – up area in 2023, 45.94 % reduction in vegetation in 2023 & 66.27 % reduction in water bodies in 2023 when compared with 1992 data. LST as observed in table - 5.3, Graphs and map data over the period of 1992 – 2023 we can see a rapid raise of temperature in summer & winter. The range of temperature in 1992 summer data were 14.70 °C - 31.50°C 11 and in the year 2023 the values were 21.53 °C - 51.23°C. 1992 winter data was 14.50 °C – 31.00 °C and in the year 2022 were 7.56 °C – 39.71 °C When the values of UTFVI were classified based on threshold values of UTFVI we can see more HOTSPOT’s in 2023 data comparing to 1992 and as we can see in Digital elevation

model the heart of the city is at a higher elevation compared to outlying areas and causing dispersion of Surface heat resulting in reduced UHI.

Table 5.1: LU/ LC of 1992 Classification

1992 Classification		
Classification	Area in sq km	Percentage
Built up	137	3.04
Vegetation	838	18.65
Water Bodies	86	1.92

Table 5.2: LU/ LC of 2023 Classification

2023 Classification		
Classification	Area in sq km	Percentage
Built up	1362	30.3
Vegetation	385	8.57
Water Bodies	57	1.26

Table 5.3: LST values from 1992-2023

Year	7 ⁰ C to 15 ⁰ C (Are in Sq km)	15 ⁰ C to 25 ⁰ C (Are in Sq km)	25 ⁰ C to 32 ⁰ C (Are in Sq km)	32 ⁰ C to 38 ⁰ C (Are in Sq km)	38 ⁰ C to 52 ⁰ C (Are in Sq km)
1992 Winter	0.71	3705.15	788.14	0	0
1992 Summer	0.013	3423.25	740.75	329.98	0
2002 Winter	0.01	177.81	4010.93	304.94	0.31
2002 Summer	1.26	9.85	652.02	3198.4	632.47
2013 Winter	0.01	1438.28	3057.38	0.23	0
2013 Summer	0	5.06	215.34	2829.45	1428.63
2022 Winter	0.1	406.64	4074.37	12.88	0.002
2023 Summer	0	0.12	191.79	2264.61	2037.48

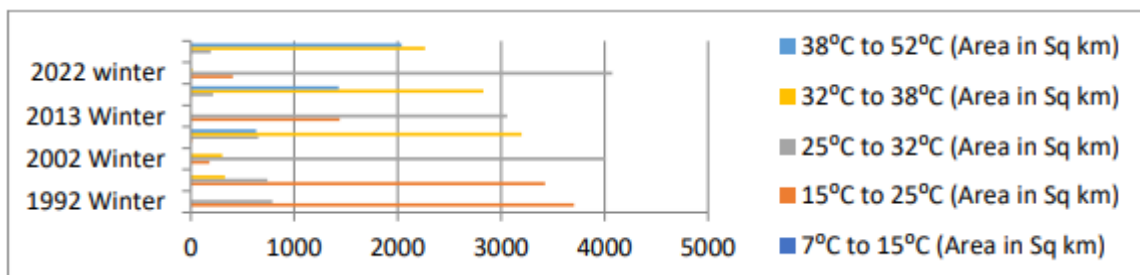


Figure 5.1.1: LST values from 1992- 2023 in graphical representation

5.2. Preventive measures

To reduce the urban heat island effect following methods can be adopted.

- Incorporate green infrastructure improvements into routine street renovations and capital improvement projects to guarantee that the city will continue to invest in heat-reducing practices.

- Plant trees and other types of vegetation. Although space may be constrained in urban areas, it is simple to incorporate small green infrastructure practices into grassy or barren areas, vacant lots, and street rights-of-way.
- To improve roadside cooling and shading, plant trees in or near planters and employ other green infiltration based strategies.
- Install green roofs-Green roofs are a great way to reduce heat islands because they cool the surrounding air directly. By absorbing pollutants and reducing the heat island effect, green roofs also improve air quality

6. Conclusion

This study has demonstrated a satellite-based method of monitoring LULC, LST & UHI effect, it shows how time series satellite imageries can be used to estimate UHI occurrence, the UTFVI which was generated from LST was used to observe the urban ecological quality of life through the connection of thermal comfort and the UHI intensity values. It is noteworthy that the region in the study area which is impacted by urban heat island effect expanded over the study period, the highest UHI rising temperatures and total amount of UHI rising temperatures show a rapid growth in the same period, for this reason, the study area experiences both severe conditions of optimal microclimate for quality urban life and the worst condition of thermal discomfort. Finally, it is evident that satellite remote sensing offers a quicker and efficient technique in the investigation of UHI as compared to the conventional in-situ method

References

- [1] Summary of current radiometric calibration coefficient for Landsat MSS, TM and EO-1 ALI sensors by Gynesh Chander. et.al.,2013
- [2] Balling, R. C. & Brazell, S. W. (1988) - High resolution surface temperature pattern in a complex urban terrain, Photogrammetric Engineering and Remote Sensing, 54, 1289-1293
- [3] Bornstein, R. D. (1987) - Mean diurnal circulation and thermodynamic evolution of urban boundary layers. Modeling the urban boundary layer, Boston, American Meteorological Society, 53-93
- [4] Karthikeyan, S. (1999) - The fauna of Bangalore – the vertebrates and butterflies of Bangalore: a checklist, Worldwide Fund for Nature-India. Karnataka State Office, Bangalore
- [5] Greater Bangalore: Emerging heat island by Ramachandra T. V. and Uttam Kumar (2010)
- [6] Remote sensing of land cover's effect on surface temperatures: a case study of the urban heat island in Bangalore, India by Shrinidhi Ambinakudige (2011)
- [7] Modeling and Simulation of Urbanization in Greater Bangalore, India Bharath H Aithal.et.al.,2013
- [8] A review on the generation, determination and mitigation of Urban Heat Island, RIZWAN Ahmed Memon.et.al., 2007
- [9] Recent challenges in modeling of urban heat island Parham A. Mirzaei 2015

- [10] Analysis of diurnal surface temperature variations for the assessment of surface urban heat island effect over Indian cities Aneesh Mathew.et.al., 2017
- [11] A study of the Urban Heat Island of Granada by Juan P. Montávez.et.al., 2000
- [12] A remote sensing study of the urban heat island of Houston, Texas by David R. Streutker 2016 13
- [13] Analysis of urban heat island in Kochi, India using modified climate zone classification by George Thomas (2013)
- [14] Estimation of Urban heat island in local climate change and vulnerability assessment of air quality in Delhi by Mina Babazadeh and Parvendra Kumar (2015)
- [15] Research on Urban Heat-island Effect by Li yang et al (2016)
- [16] A temporal study of Urban heat island Evaluation of Ahmedabad city, Gujrat Ajanta Goswami et al (2016)
- [17] Urbanization and it's impact on urban heat Island intensity in CMA by Lilly Rose Amirtham (2016)
- [18] Urban heat island modelling of tropical city, case of Kuala Lumpur by Kai wang et al (2019)
- [19] Longitudinal study of LST using mono-split windows algorithm & it's relationship using NDVI & NDBI by Shah Fahad (2020)